Structure, room-temperature magnetic and optical properties of Mn-doped TiO_2 nano powders prepared by the sol–gel process*

Ding Peng(丁 芃), Liu Fa-Min(刘发民)†, Zhou Chuang-Cang(周传仓), Zhong Wen-Wu(钟文武), Zhang Huan(张 嬛), Cai Lu-Gang(蔡鲁刚), and Zeng Le-Gui(曾乐贵)

Department of Physics, School of Physics and Nuclear Energy Engineering, Key Laboratory of Micro-nano Measurement-Manipulation and Physics (Ministry of Education), Beijing University of Aeronautics and Astronautics, Beijing 100191, *China*

(Received 19 April 2010; revised manuscript received 21 May 2010)

TiO_2 nano powders with Mn concentration of 0 at%–12 at% were synthesized by the sol–gel process, and were annealed at 500 °C and 800 °C in air for 2 hrs. X-ray diffraction (XRD) measurements indicate that the Mn–TiO_2 nano powders with Mn concentration of 1 at% and 2 at% annealed at 500 and 800 °C are of pure anatase and rutile, respectively. The scanning electron microscope (SEM) observations reveal that the crystal grain size increases with the annealing temperature, and the high resolution transmission electron microscopy (HRTEM) investigations further indicate that the samples are well crystallized, confirming that Mn has doped into the TiO_2 crystal lattice effectively. The room temperature ferromagnetism, which could be explained within the scope of the bound magnetic polaron (BMP) theory, is detected in the Mn–TiO_2 samples with Mn concentration of 2 at%, and the magnetization of the powders annealed at 500 °C is stronger than that of the sample treated at 800 °C. The UV–VIS diffuse reflectance spectra results demonstrate that the absorption of the TiO_2 powders could be enlarged by the enhanced trapped electron absorption caused by Mn doping.

Keywords: Mn-doped TiO_2 nano powders, sol–gel process, room-temperature magnetic properties, diffuse reflectance spectra

PACC: 8120E, 6116D, 7550P, 6170T

1. Introduction

Since TiO_2-based diluted magnetic semiconductor (DMS) with room temperature ferromagnetism was successfully prepared by Matsumoto *et al.*,[1] this material has been drawing rapidly increasing attention from researchers because of its potential in magneto-electronic applications.[2,3] TiO_2 doped with Fe,[4,5] Co,[6−9] V,[10,11] Cr,[12] Mn[13−18] and other elements have been prepared by PLD,[19] MBE,[20] magnetron sputtering,[7,16] ion implantation,[8,15] sol–gel,[13,17,18] and other methods.[5,9] Although ferromagnetism in Mn doped TiO_2 has been reported for several times,[13,14,16−18,21−26] few report has been given on the effect of annealing treatment on ferromagnetism and optical absorption of Mn–TiO_2 nano powders.

In this work, Mn-doped TiO_2 powders were synthesized by sol–gel process and were annealed at different temperatures in air for 2 hrs. The structure, morphology, and composition of the samples were investigated by XRD, HRTEM, SEM, and energy dispersive x-ray spectrum (EDX). The magnetic properties were measured by vibrating sample magnetometer (VSM). The diffuse reflectance spectra were taken on a UV–VIS spectrophotometer. We report herein the structure and phase transformation in the Mn-doped TiO_2 nano powders, and moreover the magnetic and optical properties of the powders are also discussed.

2. Experimental

The Mn-doped TiO_2 nano powders were synthesized by sol–gel process, and were annealed at 500 °C and 800 °C in air for 2 hrs. The process of precursor colloid is as follows. First, 1.2 ml acetic acid (CH_3COOH) and 5.7 ml titanium butoxide ($Ti[O(CH_2)_3CH_3]_4$) were dissolved into 10 ml anhydrous ethanol and mixed by stirring for 15 min to form ethanol solution A. Second, a mixture B composed by 10 ml anhydrous ethanol and 1.2 ml manganese

*Project supported by the Innovation Foundation of BUAA for PhD Graduates (Grant No. 292122) and Equipment Research Foundation of China.
†Corresponding author. E-mail: fmliu@buaa.edu.cn
© 2010 Chinese Physical Society and IOP Publishing Ltd

acetate ($(C_2H_3O_2)_2Mn{\cdot}4H_2O$) hydrosol with certain concentration was put into ethanol solution a drop by drop. Third, the solution was stirred for 30 min at 25 °C to form homogeneous colloid. After that, the colloid with varied Mn concentration was heated at 100 °C in air to form dried gel. Finally, the dried gel was annealed at 500 and 800 °C in air for 2 hrs to form Mn-doped TiO_2 nano powders. The Mn concentration is defined to be $N_{Mn}/(N_{Mn}+N_{Ti})$, and controlled by the concentration of $((C_2H_3O_2)_2Mn{\cdot}4H_2O)$ hydrosol during the synthesis process, where N_{Mn} and N_{Ti} represent the amount of the Mn and Ti atoms in a certain sample, respectively.

These powders were investigated by XRD, HRTEM, SEM, EDX, and VSM. XRD studies were carried out on an X'Pert Pro XRD system with x-ray Mirror PFX and with an operating voltage of 40 kV and a current of 40 mA. The shape of the samples and the concentration of Mn content were measured on a FEI-SIRION SEM. The amount of doping, measured by EDX, is denoted as the fraction (at %) of number of impurity atoms to the sum of those of Ti and impurity atoms in the powders. The HRTEM micrographs were obtained on a JEM-2010 TEM. The magnetic properties of the films were measured on a Lake Shore-VSM7404 VSM at room temperature. The diffuse reflectance spectra were taken on a UV–VIS spectrophotometer.

3. Results and discussion

3.1. The composition and morphology of Mn-doped TiO_2 nano powders

The Mn concentrations of the samples were measured by EDX. Figure 1 shows a typical spectrum of the Mn-doped TiO_2 nano powder sample with Mn concentration of 10 at%. The calculated Mn atom composite $N_{Mn}/(N_{Mn}+N_{Ti}) = 4.11/(4.11+35.65) = 10.3\%$ is in accordance with the designed concentration. SEM images (Fig. 2) show that the grain sizes of the powders annealed at either 500 °C or 800 °C are uniform. The diameter of the grains in Fig. 2(a) is about 10 nm and that in Fig. 2(b) is over 200 nm, which indicates that the crystal grain size increases with the annealing temperature.

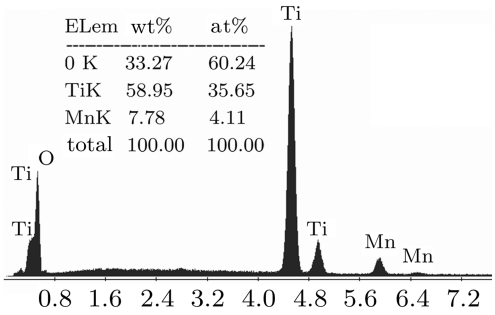


Fig. 1. EDX spectrum of the Mn-doped TiO_2 nano powder sample with Mn concentration of 10 at%.

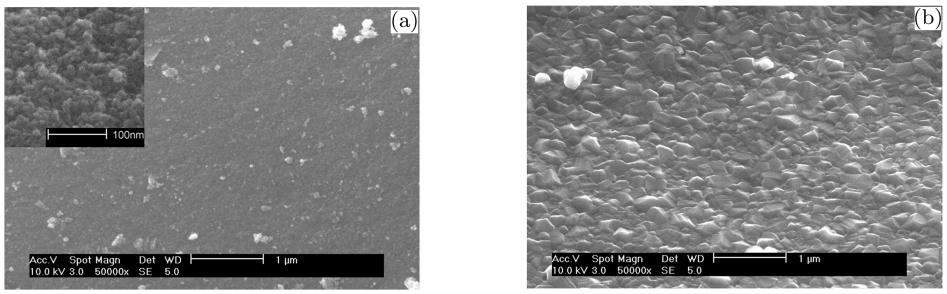


Fig. 2. SEM images of the Mn-doped TiO_2 nano powder sample with Mn concentration of 2%. (a) Annealed at 500 °C or 2 hrs, the insert shows a micrograph with high magnification for the same area; (b) Annealed at 800 °C for 2 hrs.

3.2. The structure of Mn-doped TiO_2 nano powders

Figures 3(a) and 3(b) show the XRD results of the powders annealed at 500 °C and 800 °C for 2 hrs, respectively. It is recognizable from Fig. 3(a) that the samples with the Mn concentration of 0 at%–9 at% are of anatase structure. A second phase, Mn_2O_3, appears when the Mn concentration is as high as 12%.

From Fig. 3(b), one can see that among the powders annealed at 800 °C, the un-doped ones are mixed with anatase and rutile, and the samples doped with 1% and 2% Mn are rutile structure without any second phase. The powders with Mn concentration higher than that of 2% are mixed with rutile and Mn_2O_3, and the intensity of the second phase increases with the Mn concentration.

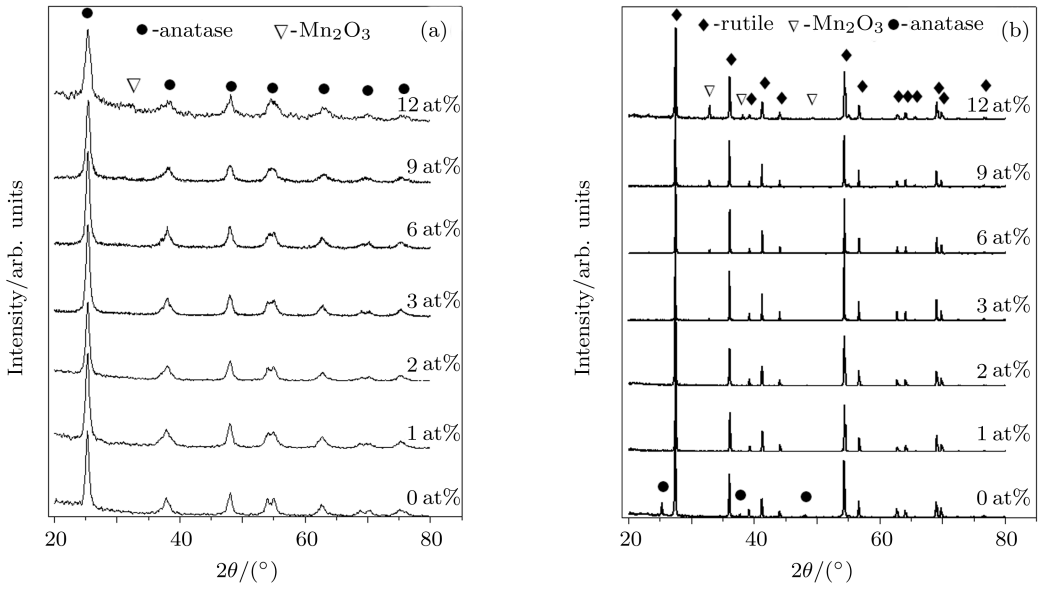


Fig. 3. XRD patterns of TiO_2 nano powders doped with Mn concentration of 0 at%–12 at% annealed for 2 hrs. (a) at 500 °C (b) at 800 °C.

It is noted that the reflection peaks in Fig. 3(a) are broadened than those in Fig. 3(b), it is because the average grain size in the samples annealed at 800 °C is larger than that of the samples annealed at 500 °C, as shown in Fig. 2. Structural analysis of the XRD data also suggest that the increase of annealing temperature for the Mn-doped TiO_2 could effectively increase phase transition from anatase to rutile in contrast with what observed in TiO_2, this fact is in agreement with that reported by Arroyo *et al.*[27]

Figure 4 shows a HRTEM micrograph of the Mn-doped TiO_2 sample with Mn concentration of 1 at%, annealed at 500 °C for 2 hrs. The insets display the selected area diffraction (SAED) pattern and the low magnification image of the powder sample. It is seen from the low magnification image that the grain size of the sample is about 10 nm, the same as the SEM results. The inter-planar spacing, 0.35 nm, is marked, and is consistent with the inter-planar distance of (101) crystal planes of anatase TiO_2. Both the HRTEM image and the SEAD pattern confirm that these powders have the anatase structure.

Figure 5 shows the HRTEM micrographs along the [001] zone axis of a crystal in the Mn-doped TiO_2 powder sample with Mn concentration of 1 at%, annealed at 800 °C for 2 hrs. The insets show the enlarged image of the smaller selected area and the fast Fourier transform (FFT) pattern of the area marked with the larger frame.

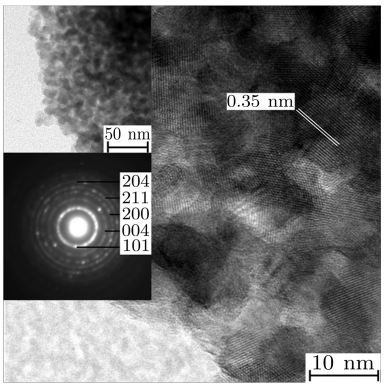


Fig. 4. HRTEM micrographs of the Mn-doped TiO_2 powder sample with Mn concentration of 1 at%, annealed at 500 °C for 2 hrs. The insets are a selected area diffraction pattern and a bright-field TEM image.

The unit cell of rutile TiO_2, as below shown in Fig. 6(a), is tetragonal ($a = b = 4.584$ Å, $c = 2.953$ Å (1 Å = 0.1 nm), space group $P42/mnm$).[26] The structure has only one crystallographic Ti site. These Ti atoms are surrounded by a slightly distorted octahedron of oxygen atoms. The Mn atoms which are expected to substitute for Ti have also one crystallographic site in the Mn–TiO_2 crystal.

The distance 0.46 nm marked in the upper insert of Fig. 5 is consistent with the lattice constant a of rutile TiO_2. It can be clearly seen that the lattice in the same graph is in agreement with that in Fig.6 (b) which is simulated by the Materials Studio software. The HRTEM images of both the powders

annealed at 500 ℃ and 800 ℃ show that the samples are well crystallized without any impurity phase being detected, indicating that Mn has doped into the TiO_2 crystal lattice effectively.

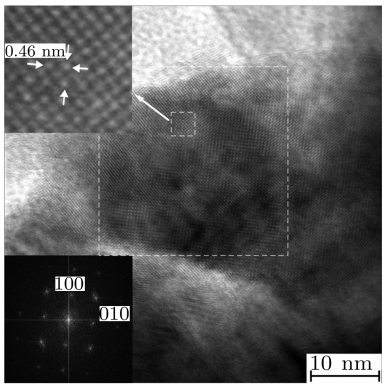


Fig. 5. HRTEM micrographs of the Mn-doped TiO_2 nano powder sample with Mn concentration of 1 at%, annealed at 800 °C for 2 hrs. The insets show the enlarged image of the rectangular area and the fast Fourier transform (FFT) pattern of the area marked with the larger frame.

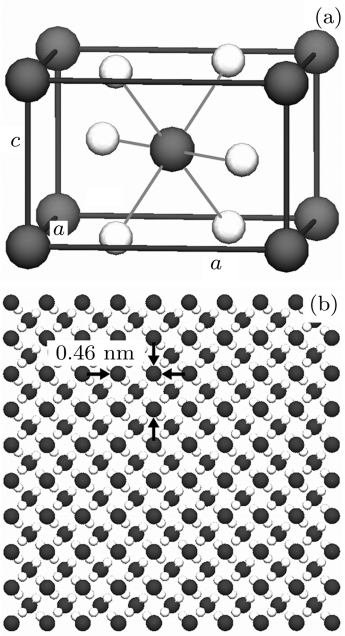


Fig. 6. The crystal lattice of rutile TiO_2 (Ti: gray balls, O: white balls): (a) unit cell; (b) along the [001] zone axis.

3.3. The room-temperature ferromagnetism and optical properties of Mn-doped TiO_2 nano powders

Figure 7 shows the room temperature hysteresis loops for Mn-doped TiO_2 powder sample with Mn concentration of 2 at%, annealed at 500 ℃ and 800 ℃ for 2 hrs, illustrating the ferromagnetism in the present samples. The magnetization of the powders annealed at 500 ℃ is visibly larger than that of the sample treated at 800 ℃.

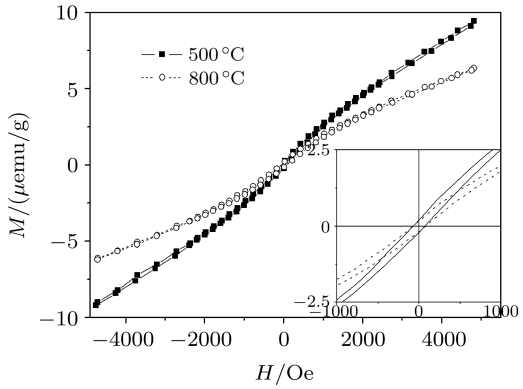


Fig. 7. The room temperature hysteresis loops for Mn-doped TiO_2 nano powder samples with Mn concentration of 2 at%, annealed at 500 °C and 800 °C for 2 hrs. The inset shows the low-field part of the loops for the two samples (1 Oe = 79.5775 A/m).

As mentioned above, the XRD and HRTEM results confirm that Mn has effectively doped into the crystal lattice of TiO_2. On the other hand, oxygen vacancies in TiO_2[28,29] could be produced by annealing treatment. The ferromagnetism (FM) in Mn doped TiO_2 have been reported for anatase[13] and rutile[17] and explained within the scope of the bound magnetic polaron (BMP) theory.[30] When the concentration of shallow defects exceeds the percolation threshold, defects such as oxygen vacancies can overlap many doped ions to yield BMPs, which can result in FM coupling between doped spins. Xu *et al* discovered that the ferromagnetism was enhanced as the phase transition from anatase to rutile occurs.[22] In their experiment, the annealing temperatures for anatase and mixed phase were almost the same. But in the case of the present work, the annealing temperature (800 °C) to obtain rutile is much higher than that of anatase (500 °C). When the samples are annealed under high temperature in air, the oxygen deficiency could be reduced because some oxygen vacancies would be generally diminished or eliminated. As a result, the magnetization of the powders annealed at 500 °C is larger than that annealed at 800 °C.

Figure 8 shows the diffuse reflectance spectra of the undoped and Mn-doped TiO_2 powders. Figure 8(a) shows an absorption tail in the 350–450 nm region. According to the equation (1).[31] The reflectance data $R\%$ were converted into Kubelka–Munk function $F(R)$, which is proportional to the absorption coefficient α.

$$F(R) = \frac{(1-R)^2}{2R}. \quad (1)$$

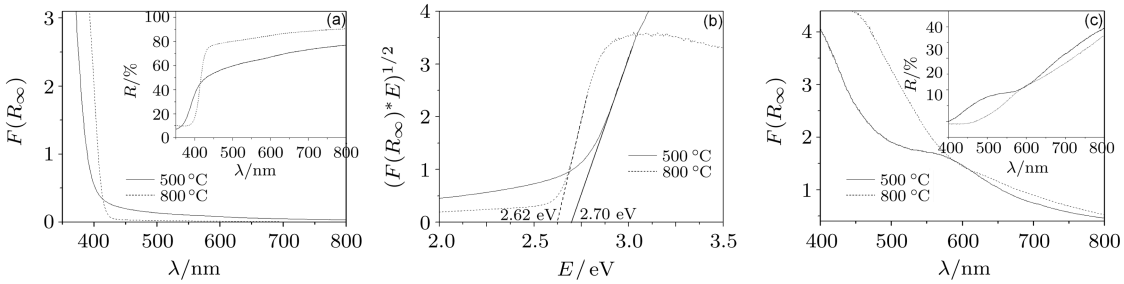


Fig. 8. Diffuse reflectance spectra (a) TiO_2 samples annealing at different temperatures, insert shows the original reflectance data $R\%$ curve; (b) Transformed Kubelka–Munk function vs. excitation energy for pure TiO_2 samples; (c) Mn-doped TiO_2 nano powders with Mn concentration of 2 at% annealing at different temperatures, insert shows the original reflectance data $R\%$ curve.

And the absorption coefficient α of an indirect semiconductor near the absorption threshold can be expressed as:

$$\alpha = \frac{B_{\rm i}(E - E_{\rm g})^2}{E}, \tag{2}$$

where $E_{\rm g}$ is the band gap of indirect allowed transition (eV), E is the energy of the light (eV), B_i is the absorption constant. Therefore, the transformed Kubelka–Munk function can be constructed by plotting $[F(R)*E]^{1/2}$ values against excitation energy and allows to evaluate the band gap energy.[32] It can be evaluated from Fig. 8(b) that the $E_{\rm g}$ of the undoped TiO_2 powders annealed at 500 °C is 2.70 eV, bigger than that of at 800 °C, 2.62 eV, because the $E_{\rm g}$ of anatase is bigger than that of rutile.

Figure 8(c) shows the diffuse reflectance spectra Mn-doped TiO_2 nano powders with Mn concentration of 2% annealing at different temperatures. One can see that the reflectance data $R\%$ of the powders annealed at 500 °C and 800 °C are low over the visual region, indicating that the absorption of samples is large because of the Mn doping. A broad peak at about 560 nm for the powders annealed at 500 °C can be seen in Fig. 8(c). Compared with the reported literatures,[33,34] this peak may be ascribed to the enhanced trapped electron absorption caused by the doped Mn ions.

4. Conclusions

In summary, TiO_2 nano powders doped with Mn concentration ranging from 0 at% to 12 at% were synthesized by sol–gel process and were annealed at 500 °C and 800 °C in air for 2 hrs. Both the XRD patterns and HRTEM images confirm that Mn has doped into the TiO_2 crystal lattice effectively. Ferromagnetism is detected in the Mn–TiO_2 powders and could be understood as BMP enhanced ferromagnetism. Mn doping can enlarge the absorption of the TiO_2 powders by means of enhanced trapped electron absorption.

References

[1] Matsumoto Y, Murakami M, Shono T, Hasegawa T, Fukumura T, Kawasaki M, Ahmet P, Chikyow T, Koshihara S and Koinuma H 2001 *Science* **291** 854

[2] Zutic I, Fabian J and Das Sarma S 2004 *Rev. Mod. Phys.* **76** 323

[3] Wu S X, Li X Y, Xing X J, Hu P, Yu Y P and Li S W 2009 *Appl. Phys. Lett.* **94** 253504

[4] Xu J P, Li L, Lü L Y, Zhang X S, Chen X M, Wang J F, Zhang F M, Zhong W and Du Y W 2009 *Chin. Phys. Lett.* **26** 097502

[5] Sangaletti L, Mozzati M C, Drera G, Galinetto P, Azzoni C B, Speghini A and Bettinelli M 2008 *Phys. Rev.* B **78** 075210

[6] Akdogan N, Nefedov A, Zabel H, Westerholt K, Becker H W, Somsen C, Gök Ş, Bashir A, Khaibullin R and Tagirov L 2009 *J. Phys.* D: *Appl. Phys.* **42** 115005

[7] Mi W B, Jiang E Y and Bai H L 2009 *J. Magn. Magn. Mater.* **321** 2472

[8] Liu F M, Ding P, Yang X A and Li J Q 2009 *Nucl. Instr. Meth.* B **267** 3104

[9] Yan W S, Sun Z, Pan Z Y, Liu Q H, Yao T, Wu Z Y, Song C, Zeng F, Xie Y N, Hu T D and Wei S Q 2009 *Appl. Phys. Lett.* **94** 042508

[10] Huang D, Zhao Y J, Chen D H and Shao Y Z 2009 *J. Phys.*: *Condens. Matter.* **21** 125502

[11] Wen Q Y, Gu D E, Zhang H W, Yang Q H, Li Y X, Liu Y L and Xiao J Q 2009 *J. Phys.* D: *Appl. Phys.* **42** 055012

[12] Li J, Song G B, Wang M L and Zhang B S 2007 *Acta Phys. Sin.* **56** 3379 (in Chinese)

[13] Bhattacharyya S, Pucci A, Zitoun D and Gedanken A 2008 *Nanotechnology* **19** 495711
[14] Tian Z M, Yuan S L, Wang Y Q, He J H, Yin S Y, Liu K L, Yuan S J and Liu L 2008 *J. Phys.* D: *Appl. Phys.* **41** 055006
[15] Ding P, Liu F M, Yang X A and Li J Q 2009 *Nucl. Instr. Meth.* B **267** 3109
[16] Ding P, Liu F M, Yang X A and Li J Q 2008 *Chin. Phys.* B **17** 0721
[17] Kim K J, Park Y R, Lee J H, Choi S L, Lee H J, Kim C S and Park J Y 2007 *J. Magn. Magn. Mater.* **316** e215
[18] Xu J P, Wang J F, Lin Y B, Liu X C, Lu Z L, Lu Z H, Lü L Y, Zhang F M and Du Y W 2007 *J. Phys.* D: *Appl. Phys.* **40** 4757
[19] Hong N H, Sakaib J, Prellierc W and Ruyter A 2005 *Physica* B **355** 295
[20] Osterwalderb J, Droubaya T, Kaspara T, Williamsa J, Wanga C M and Chambers S A 2005 *Thin Solid Films* **484** 289
[21] Wang Z J, Tang J K, Chen Y X, Zhang H G, Golub V, Spinu L and Tung L D 2004 *J. Appl. Phys.* **95** 7384
[22] Xu J P, Lin Y B and Lu Z H 2006 *Solid State Commun.* **140** 514
[23] Hong N H 2006 *J. Magn. Magn. Mater.* **303** 338
[24] Cabrera A F, Errico L, Rodr´iguez Torres C E and Sánchez F H 2007 *Physica* B **389** 103
[25] Li X Y, Wu S X, Xu L M, Li C T, Liu Y J, Xing X J and Li S W 2009 *Mater. Sci. Eng.* B **156** 90
[26] Errico L A, Rentería M and Weissmann M 2005 *Phys. Rev.* B **72** 184425
[27] Arroyo R, Cordoba G, Padilla J and Lara V H 2002 *Mater. Lett.* **54** 397
[28] Nowotny J, Padecka M and Rekas M 1997 *J. Phys. Chem. Solids* **58** 927
[29] Bak T, Nowotny J, Rekas M and Sorrell C C 2003 *J. Phys. Chem. Solids* **64** 1057
[30] Coey J M D, Venkatesan M and Fitzgerald C B 2005 *Nature Mater.* **4** 173
[31] Simmons E L 1974 *Appl. Opt.* **14** 1380
[32] Lin H, Huang C P, Li W, Ni C, Shah S I and Tseng Y H 2006 *Appl. Catal.* B **68** 1
[33] Xu L M, Xing X J, Yang M, Li X Y, Wu S X, Hu P, Lu J Q and Li S W 2010 *Appl. Phys.* A **98** 417
[34] Pan D Y, Wan J G, Xu G L, Lü L Y, Wu Y J, Min H, Liu J M and Wang G H 2006 *J. Am. Chem. Soc.* **128** 12609